Rui Yin[1*],
Yaqian Dai[2]

Artwork Traceability and Anti-Counterfeiting Model Based on Block Chain Technology

Journal of Electrical Systems

Abstract: - The Chinese art market fostered the advancement of culture and spirituality. Nevertheless, false and counterfeit artwork is not uncommon. The art technology and security introduce the innovative method to determine Artwork Traceability and Anti-Counterfeiting. The aim of the work is to prevent the creation and circulation of fake or unauthorized copies of artworks. Because of the cryptographic security and immutability of block chains, it would be challenging to falsify artwork records or make accurate duplicates. This would foster confidence in the art market and shield collectors and artists from monetary losses and harm to their reputations. The data on mobile Application Data Center (ADC) platform and the cleansing the data using sub-aperture keystone transform matched filtering (SAKTMF) and the preprocessed data is fed into the Hierarchically Gated Recurrent Neural Network (HGRNN) classify the art work and Anti-Counterfeiting. The Bald Eagle Search Optimization (BES) Algorithm is used to optimize the weight parameter of HGRNN. The proposed model is implemented in MATLAB/ Simulink platform and the accuracy is compared to various existing approaches such as Dual-Branch Multi-Scale Feature Fusion network (DMF-Net), Region Convolutional Neural Network (R-CNN) and practical Byzantine fault tolerance (PBFT) algorithm. The gained results of the proposed HGRNN-BES method attains higher accuracy 97%, 96%, and 99%, higher precision 98%, 99%, and 97%.

Keywords: Artwork Traceability, Anti-Counterfeiting, Art market, Block Chain, Supply Chain Management.

I. INTRODUCTION

Block chain technology [1], which has gained attention recently, has advanced extremely quickly. Because of its decentralized and tamper-proof nature, block chain-based traceability systems offer an answer to the drawbacks of conventional traceability systems. An RFID and block chain-based supply chain tracking solution for agricultural products [2, 3]. Information traceability along the whole agricultural products supply chain was made possible by the collection, sharing, and transmission of actual data on the production, processing, warehousing, distribution, and sales of agricultural commodities [4, 5]. Although the former included anti-counterfeiting substance in packing materials, customers still find it difficult to tell the difference between real and phony goods in real-world situations. The most popular type of anti-counterfeiting labels are those that use high-technology and digital anti-counterfeiting labels. Customers using digital anti-counterfeiting labels called or texted the code numbers on the labels to confirm their validity, then compared the results to the records.

Anti-counterfeiting technology's two main functions are to: (1) make it harder for counterfeiters to replicate codes [6, 7]; and (2) make it simple for consumers to verify authenticity. A program for the prevention of counterfeiting and authenticity of ceramic artworks was created utilizing two-dimensions in relation to the characteristics of ceramic art production and marketing [8, 9]. There is fierce competition among brands, a plethora of counterfeit items available, frequent prohibitions against the sale of counterfeit goods, and an approximated high amount of commerce in counterfeit goods overall. Furthermore, as counterfeit goods negatively impact customers' and brands' interests, tarnish the reputation of the whole consumer market, and hinder the industry's ability to grow sustainably, product anti-counterfeiting has gained prominence [10]. Taking a quantitative approach to the problem of counterfeiting, the amount of counterfeit goods traded internationally accounted for billions of US dollars of the global trade market [11, 12].

The purpose of block chain was to address the issue of dispersed nodes agreeing on a state without the need for a coordinating third party [13, 14]. Block chain-based traceability may track and trace the origin of products, identify counterfeit goods or fraudulent transactions, and facilitate work processing all at once [15, 16]. The goal of the anti-counterfeiting strategy is to shield customers against phony goods that can be harmful. First, a plaintext sequence was assembled using the artist's information [17], the title of the artwork, the location and date of production, and an arbitrary order.

[1] School of Culture and Arts, Zhe Jiang Technical Institute of Economics, Hangzhou, Zhejiang, 310018, China
[2] Software Development Department, Fujitsu Consulting (Canada), Vancouver, British Columbia, V3B 6P9, Canada
*Corresponding author e-mail: 290144@zjtie.edu.cn

In order to produce a succession of anti-counterfeiting sequences, the sequence was then encrypted. Lastly, anti-counterfeiting graphical two-dimensional blocks were created [18] using two-dimensional coding, and these blocks functioned as anti-counterfeiting labels for the artists' creations.

Major contribution to this work summarized here;

- Block chain technology to enable traceability and prevent counterfeiting of artwork. HGRNN is a capture hierarchical dependencies and long-term dependencies in sequential data
- HGRNN can be used to classify and verify the authenticity of artwork based on various features and characteristics. HGRNN technique enhances the security and trustworthiness of the art market.
- The power of block chain technology and the classification capabilities of the HGRNN model to enhance the security and trustworthiness of the art market.
- Customers may quickly and efficiently certify artwork using a phone by using a dynamic encryption security sequence that was developed with art-related information and a random code.

The following describes how the job is organized: The new study effort and its background are explained in Sector 2. The proposed method is described in Sector 3. The results are established in Sector 4, and the manuscript is concluded in Sector 5.

II METHODOLOGY

Numerous studies that were previously published in the literature and were based on the art work traceability and anti-counterfeiting model based on block chain technology. Among those examined were the following:

Guoet al. [19] have suggested that authentic anti-counterfeiting QR codes, but because copiers came in a variety of manufacturers and types, it was very challenging to pinpoint the specific person who copied the falsified code. To address these problems, this study suggested a deep learning-based method for identifying copy forgeries in anti-counterfeiting QR codes. An analysis of the anti-counterfeiting QR code manufacturing concept and the conversion of copy forgery detection to device category forensics led to the development of a Dual-Branch Multi-Scale Feature Fusion network. A thorough examination of the single-branch design, data preprocessing layer, and other aspects is carried out as the network is being designed.

Daoudet al. [20] have suggested that to lower the amount of fake goods by utilizing technology based on machine learning. Machine learning-based classification and picture and text recognition using R-CNN may become vital tools in the fight against counterfeiting. By comparing images with trained models, image recognition and product information categorization enable the end user to quickly and accurately identify counterfeit items. This study's goal was to create an approachable, elegant, and straightforward application that will enable end users to recognize fake goods and so aid in the battle against product piracy. Although the number of counterfeit goods on the US and European markets is rising, consumers can still help to improve the situation by taking small steps to report suspicious products to authorities and inspection agencies. Investigate the prospect of reducing counterfeit goods with machine learning-based technology in this article. Machine learning-based categorization and image and text recognition could emerge as critical technologies in the war against counterfeiting. Image recognition and product information categorization allow the end user to rapidly and correctly detect counterfeit products by comparing photos with trained models.

Tan et al. [21] have suggested that the Block chain's transparency, decentralization, anonymity, and other features made it a good fit for traceability and anti-counterfeiting applications. This article discusses the benefits and drawbacks of the standard algorithms and block chain types used in blockchain technology. In order to lower energy consumption and boost the effectiveness of supply chain anti-counterfeiting traceability systems, this study proposed a model based on the practical Byzantine fault tolerance (PBFT) algorithm of alliance chains. In this design, a credit evaluation system and a consensus mechanism are merged to determine the principal node of the weightage to contributors (WtC) method.

Mohitet al. [22] have suggested It was projected that the supply chain industry will make substantial use of blockchain technology. Traceability and ownership monitoring are still major challenges in a typical supply chain. Block chains can reduce intermediaries, boost traceability, and boost trust in the supply chain. However, it increases supply chain transparency, which brings up privacy concerns. This study suggested a unique approach to transaction privacy that takes traceability and ownership into consideration. The suggested method maintains the advantages of block chains and centralized database servers. The suggested approach makes it easier for the goods to be transferred and enables its owners to locate it. It protects the supply chain from counterfeit goods.

Alzahrani and Bulusu [23] have developed that a brand-new, fully decentralized consensus mechanism that, in contrast to the majority of current protocols, doesn't require passwords and uses a random assortment of validates with varying sizes each time a new block is proposed. Our approach assesses the danger likelihood of the block's proposing nodes using a game theoretical model. The number of validators that participated in the consensus process was decided using this risk likelihood. Furthermore, the game model penalizes dishonest players and rewards honest ones, hence enforcing the behavior of the honest consensus nodes.

Rajesh [24] have developed that A block chain-based anti-counterfeiting traceability system can guarantee the consistency and correctness of the data kept by each participating node, safeguard the data's legitimacy, guarantee the quality of the product, increase businesses' credibility, and increase consumers' faith in their offerings. Nevertheless, the integration of block chain with the conventional anti-counterfeiting traceability mode has various issues, including low efficiency, because of the restricted system throughput, high energy consumption, and inadequate data availability. The goal of this research is to develop a better contribution-proof consensus method that will increase the mining productivity of trustworthy miners.

A. Background of the Recent Research Work

A general overview of current research indicates that the anti-counterfeiting concept and artwork traceability are crucial. Block chain-based traceability may be used to detect fraudulent or counterfeit transactions. One of the most difficult tasks in art is ensuring the traceability of artwork and detecting counterfeiting. The primary characteristic of anti-counterfeiting technology is to increase the difficulty of code replication for counterfeiters. Although the former included anti-counterfeiting substance in packing materials, customers still find it difficult to tell the difference between real and phony goods in real-world situations. The most popular type of anti-counterfeiting labels are those that use high-technology and digital anti-counterfeiting labels. Numerous researchers are addressing this issue with various approaches found in literature, including as PBFT, R-CNN, and DMF-Net. Although DMF-Net provides superior results for art traceability, it is not as accurate in categorization as R-CNN, which has been shown to be highly accurate but has limited sensitivity, and PBFT, which has a significant prediction error. These issues and disadvantages have spurred me to conduct this investigation.

III. PROPOSED METHODOLOGY

The architecture of the proposed artwork traceability and anti-counterfeiting is displayed in Figure 1. Information gathered from mobile ADC platform, which may include information on environmental conditions, growth metrics or other agricultural parameters. This dataset includes the name of the artist, the piece of art, the production time and location, and a random sequence. Initially, Pre-processing is done to cleanse the data and the features are extracted. Finally, the fair artwork is detected by the classification by using HGRNN. The HHGRNN classifies the provenance, authority, and ownership based on the data. It helps to detect the fake artworks and anti-counterfeiting. The accuracy is improved by optimizing the weight of HGRNN using BES. This model improves the accuracy of the system with minimum error values.

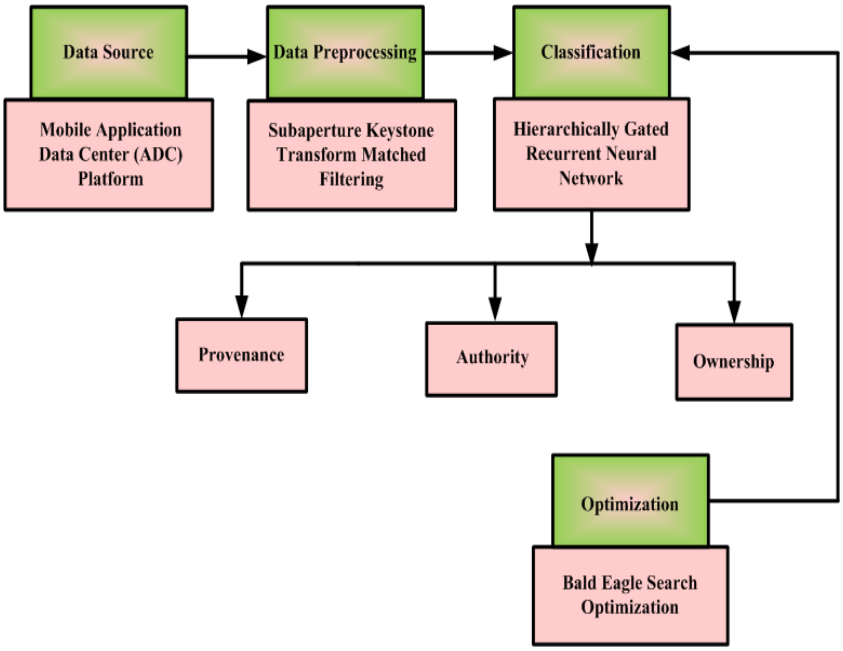

Figure 1: Proposed methodology diagram of artwork traceability and anti-counterfeiting

A. Block Chain Based Art work Traceability and Anti Counterfeiting

Blockchain-based Supply chains, products, and counterfeit items may all be tracked and traced using traceability [25]. The use of block chain technology in the arts a number of purposes, such as confirming provenance and authenticity, enabling direct communication between purchasers and artists, allowing artists to receive royalties through smart contracts, and permitting the creation and exchange of works of art. The non-tamperable change of the data on the block chain is used to remove the malicious operation of bogus artwork by a crucial third party in the storage and sharing process. The primary target audience for the blockchain-based art work security traceability system is artists, carriers, and buyers. Chain codes are used to permanently preserve manufacturing and transit data for art work products on the block chain. After making an online purchase at the mall, customers scan the QR code on the artwork to follow it through the applet. It allows for the intricacy of an economic system and provides pluggables of many components.

B. Data Acquisition

China Mobile unveiled the Application Data Center (ADC), a platform for apps for the mobile information sector [26]. At the moment, a large portion of the business focuses on wireless sites, mobile email, mobile OA, and application hosting solutions for mobile invoicing. Small and medium-sized businesses will host their own data and information on the mobile ADC platform as Group clients. For enterprises and the general public, mobile corporations provide data applications, billing management, and data access services based on websites or mobile phones. The data set is put together into a plaintext sequence and includes the name of the artist, the artwork, the production time and location, and a random sequence.

C. Pre-processing using Sub Aperture Keystone Transform Matched Filtering (SAKTMF)

The data is pre-processed using SAKTMF in this part [27]. The data is cleaned up by data processing. These data are collected from ADC and then pre-processed, mainly through text retrieval. If the data is sensitive, make sure it's properly secured and that only people with permission may access it. Based on the phase connection derivation among sub apertures, a unique SAKTMF method is created. Thus the aperture is given by the eqn. (1)

$$QR(k_t, k_n) = \sum_{l=1}^{L} QR_l(k_t, k_{n,l}) \quad (1)$$

Where, QR represents the whole data, (k_t, k_n) denotes the demodulation operation, L indicates the sub blocks and l represents the sub aperture index. Then the Doppler direction of the information data is given by the eqn. (2)

$$qR_l(k_t,h_n) = SA_{kn}\left[qr_l(k_t,k_n,l)\right] (2)$$

Here, SA_{kn} represents the performing operation with respect to k_n, h_n signifies the Doppler frequency. SAKTMF is the process of creating fresh dataset instances while maintaining correct labels when there is a shortage of labeled data. Making invariant predictions by spanning many perspectives of the same scene is the primary objective of SAKTMF. Then, it is given in eqn. (3)

$$W\{\alpha\} = \sum_{l=1}^{L}\left| qR_l\left(\frac{2}{a}t(\alpha,lD_a), h(\alpha,lD_a\right)\right| (3)$$

Here, α represents the vector in search parametric space, $t(\alpha,lD_a), and\ h(\alpha,lD_a)$ represents the Doppler location and range associated with sub aperture index l. Then, every frame is resized by the eqn. (4)

$$\left(\frac{h_a}{h_t+h_a}\right)^k \approx 1-k\frac{h_t}{h_a} (4)$$

Where, h_t represents the range frequency variable, h_a denotes the preliminary integration, k indicates the linear range. SAKTMF is deleting the wrong words, sentences, and grammar by calculating the eqn. (5)

$$\hat{y}_1 = -\frac{2}{\lambda}\left[\arg\max\{SAKTMF(k_t,h_n;\hat{y})\}\right] (5)$$

Here, $\hat{y}$ represents the corresponding searching motion parameters vector, k_t denotes the demodulation operation, λ and represents the data. Finally, the data is pre-processed by SAKTMF, which is cleanses the data. These pre-processed data are fed into the HGRNN.

D. Classification based Hierarchically Gated Recurrent Neural Network (HGRNN)

The Deep neural networks are different from ordinary neural networks. We present a fast and flexible neural network namely HGRNN [28].The several stacked layers of a hierarchically gated recurrent neural network are composed of a channel mixing module (GLU) and a token mixing module (HGRU) (gated linear unit). A basic gated linear recurrent linear unit is described as follows: the first layer, a reversible down sampling operator, reshapes the data into down sampled sub-images. We also combine the down-sampled sub-images with a configurable noise level map. HGRU investigation: A basic gated linear recurrent layer is described as follows:

$$F_T = Sigmoid\left(Z_T\ M_F + A_F\right) \in D^{1\times F} (6)$$

$$J_T = Sigmoid\left(Z_T\ M_J + A_J\right) \in D^{1\times F} (7)$$

Here F_T and J_T represent forget and input gates respectively.

Complex valued recurrence: To get element-wise linear recurrence for linear RNNs with static decay rates, Eigen decompositions are frequently carried out on the recurrent weight matrix. The expressiveness of the model is limited if only real-valued Eigen values are permitted, as this narrows the recurrent weight matrix's range and makes it symmetric. On the one hand, we extract deep coarse characteristics using layer. The first layer, where c is the image's channel number, is 64-filtered and uses a size of 3×3×c to convert noisy pictures into linear features. If the input is a grayscale picture, then c = 1; if not, then c = 3. Next, we utilize the 3 × 3 kernel size to accommodate the HGRN procedure and produce a coarse feature.

For the input G_T, we individually parameterize its imaginary and real portions as follows:

$$\mathrm{Re}\ (G_T) = SiLU\left(Z_T\ M_{GR} + A_{CR}\right) \in D^{1\times F} (8)$$

$$\mathrm{Im}\left(G_T\right) = SiLU\left(Z_T\ M_{Gj} + A_{Cj}\right) \in D^{1\times F} (9)$$

Lower bound on forget gate values: The magnitude argument λ_T is the sole factor that influences how much information is remembered. In practical terms, parameterizing lower limits separately or for every hidden state, with E being the number of layers. Considering that P is the layer index, the following calculations are expressed as follows;

$$Q = \left(Soft\max\ (\Gamma, \dim = 0) \in D^{E\times F}\right) (10)$$

$$\gamma^P = \left[Cumsum\left(Q, \dim = 0\right)\right] p \in D^{1\times F} (11)$$

Lastly, the parameterization of λ_T in the P-th layer is as follows:

$$\mu_T = Sigmoid\left(Z_T\ M_\mu + A_\mu\right) \in D^{1\times F} \quad (12)$$

In order to get the same forget rate value $\bar{\gamma}$ closed to one, the sigmoid activation function's saturated areas will push μ_T away from them.

$$\mu_T = \frac{\bar{\gamma} - \gamma^p}{1-\gamma^p} < \bar{\gamma} \quad (13)$$

Consider using leaky units and trying to input and forget gates: Using leaky units can help reduce the amount of parameters. Exponential moving averages and the discretization of continuous time systems are closely related to these units, which show empirical success.

$$E_T = \lambda_T\ \Theta \exp\left(j\theta\right) \Theta\, E_{T-1} + \left(1-\lambda_T\right) \Theta\, G_T \in \subset^{1\times F} \quad (14)$$

Here Θ denotes the element wise product. Projections and output gates: In state space models, it has been demonstrated that adding gates to the recurrence layer's output is advantageous. Before performing the output projection to obtain HGRU, an output gate is applied in the following manner. By extracting diverse aspects of noise and obtain a more comprehensive representation of the objects in the scene.

$$k_T = Sigmoid\left(M_k\ Z_T + A_k\right) \in D^{1\times 2r} \quad (15)$$

By eliminating the gradient disappearance issue and facilitating the reuse of noise features, HGRNN enhances the impact of noise reduction. However, HGRNN is nearly 3 times faster and is more memory-friendly than the existing techniques. As a result, by performing classification based on the art work and counterfeiting data. HGRNN classifies provenance, authority and ownership. Based on the classification detect and avoid fake copies. HGRNN the significantly improves efficiency while classification performance. The performance of the HGRNN is improved by optimizing the activation function by BES.

E. Bald Eagle Search Optimizer (BES)

The BES algorithm is a revolutionary meta-heuristic optimization algorithm that draws inspiration from nature. Its design is modeled after the hunting strategy or socially intelligent behavior of bald eagles during their fish-hunting [29]. The three primary phases of operation that make up the BES algorithm's working principle are the prey phase, the search phase, and the selection phase. Figure 2 depicts the flowchart of bald eagle optimizer.

Step 1: Initialization

Set the input parameters, such the voltage of the battery, to zero.

Step 2: Random Generation

According to, the input parameter is generated in matrix form at random.

$$e = \begin{bmatrix} Y_{11} & Y_{12} & Y_{13} \\ Y_{21} & Y_{22} & Y_{23} \\ Y_{31} & Y_{32} & Y_{33} \end{bmatrix} \quad (16)$$

Where, e indicates the random generation and Y indicates the system parameters.

Step 3: Calculation of fitness value

The fitness is evaluated which is described by,

$F = Optimization\ (\gamma^P)$

Step 4: Selection Phase

The bald eagles randomly choose the search region at first, then assess the prey to determine the optimal location. At this point, the location is mostly assessed using a priori knowledge and parameters that change with location, which are stated as follows in Eqn. (17)

$$D_m^{s+1} = D_{best} + \beta * \alpha * \left(D_{mean} - D_m^s\right) \quad (17)$$

Where δ is the random number in range [0,1], β is the control parameter for change in position varying from 1.5 to 2, and D_m^{s+1} is the location of the m^{th} bald eagle search agent at $(s+1)^{th}$ iteration. The best position reached by bald eagles is D_{best}, and all the data from previous positions that eagle search agents employ is represented by D_{mean}.

Step 5: Search Phase

The bald eagle's search agents seek for their prey in a spiral motion that speeds up the search and determines the best place for a dive catch. Eqns. (18)–(22) express the location based on this procedure.

$$D_m^{s+!} = D_m^s + a(m) * \left(D_m^s - D_{mean}\right) + b(m) * \left(D_m^s - D_m^{s-1}\right) \quad (18)$$

$$a(m) = \frac{ag(m)}{\max(|ag|)} \text{ and } b(m) = \frac{bg(m)}{\max(|bg|)} \quad (19)$$

$$ag(m) = g(m) * \sin\theta(m) \text{ and } bg(m) = g(m) * \cos\theta(m) \quad (20)$$

$$g(m) = \theta(m) + H * Random \quad (21)$$

$$\theta(m) = \nu * \pi * Random \quad (22)$$

In this case, $g(m)$ denotes the spiral equation's polar diameter and $\theta(m)$ denotes its polar angle. H is a value that ranges from 0.5 to 2 and ends the search cycles. The random number $Random$ is between 0 and 1, and the polar coordinates of the bald eagle search agents are represented by $a(m)$ and $b(m)$.

Step 6: Prey Phase

The other members of the population approach the optimum area and launch an attack as the bald eagle searchers go down from the ideal spot in the direction of their target. Equations formulate the location at this stage of action. (23)–(27).

$$D_m^{s+1} = Random * D_{best} + a_1(m) * \left(D_m^s - f_1 * D_{mean}\right) + b_1(m) * \left(D_m^s - f_2 * D_{best}\right) \quad (23)$$

$$a_1(m) = \frac{ag(m)}{\max(|ag|)} \text{ and } b_1(m) = \frac{bg(m)}{\max(|bg|)} \quad (24)$$

$$ag(m) = g(m) + \sin\theta(m) \text{ And } bg(m) = g(m) * \cos\theta(m) \quad (25)$$

$$g(m) = \theta(m) \quad (26)$$

$$\theta(m) = \nu * \pi * Random \quad (27)$$

The workout intensities of bald eagles to the optimal and center position are denoted by f_1 and f_2, which hold the measure in range.

Step 7: Updation Phase

Lower fitness ratings are disregarded and the bald eagles are ranked based on their capacity assessments. If the current fitness metric is not the best fit, the previous choice is still regarded as the optimal result.

Step 8: Termination Phase

Once the necessary number of iterations has been completed to get the best result, the process is terminated. Hence the activation function of HGRNN is optimized by the BES.

IV. RESULT AND DISCUSSION

The experimental result of the art work traceability and anticounterfeiting using HGRNN-BES based on block chain technology. MATLAB/Simulink is used to conduct the simulations. MATLAB is used to simulate the proposed method under various performance criteria. Results of HGRNN-BES examined using DMF-Net, RCNN, and PBFT, three of the current methodologies.

A. Metric Performance Measures

The efficiency is determined to assess the model's performance. Metrics are employed in measuring. Any model will assess the output of the pattern in relation to these metrics. True Positive (TP): It's the percentage of true positives that are expected to be positive.

- True Negative (TN): It is the proportion of real negatives expected to be negative.
- False Positive (FP): It is the proportion of fake positives expected to be positive.

- False Negative (FN): It is proportion of fake negative expected to negative.

1) Accuracy

It is total accurate degree or grouping accuracy, represented in Eqn. (28),

$$Accuracy = \frac{TP + TN}{TP + FP + TN + FN} \quad (28)$$

2) Precision Rate

The precision rate is represented in Eqn. (29),

$$\Pr ecisionrate = \frac{pt}{(tp + fp)} \quad (29)$$

3) Error Rate

Error rate is represented as in Eqn. (30),

$$error\,rate = 100 - accuracy \quad (30)$$

4) Sensitivity

Sensitivity is represented as in equation (31),

$$Sensitivity = \frac{TP}{TP + FN} \quad (31)$$

5) Specificity

Specificity is represented as in equation (32),

$$Specificity = \frac{TN}{TN + FP} \quad (32)$$

The accuracy of the DMF-Net approach is established as 72% in provenance and 81% in authority and 82% in ownership. The accuracy of R-CNN is analyzed as 82% in provenance and 60% in authority and 61% in ownership. The accuracy of PBFT is analyzed as 78% in provenance and 62% in authority and 80% in ownership. In our proposed method HGRNN-BES is 97% in provenience and 96% in authority and 99% in ownership it is displayed in Figure 2. The precision of the DMF-Net approach is established as 72% in provenance and 70% in authority and 71% in ownership. The precision of R-CNN is analyzed as 79% in provenance and 70% in authority and 68% in ownership. The precision of PBFT is analyzed as 79% in provenance and 70% in authority and 60% in ownership. In our proposed method HGRNN-BES obtains 98% in provenience and 99% in authority and 97% in ownership it is shown in Figure 3.The error rate of the DMF-Net approach is established as 25% in provenance and 20% in authority and 20% in ownership. The error rate of R-CNN is analyzed as 17% in provenance and 39% in authority and 36% in ownership. The error rate of PBFT is analyzed as 22% in provenance and 33% in authority and 20% in ownership. In our proposed method HGRNN-BES obtains 2.5% in provenience and 2% in authority and 1.5% in ownership it is shown in Figure 4.

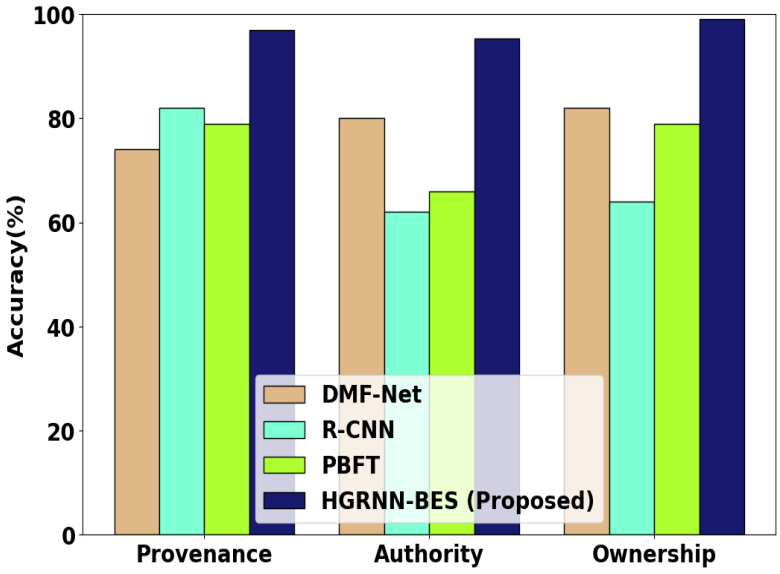

Figure 2: Accuracy of HGRNN-BES and existing approaches

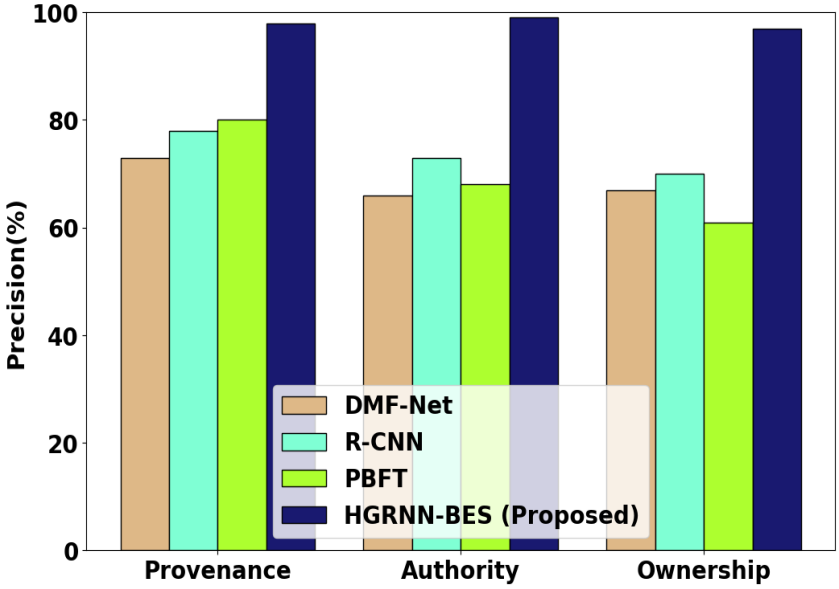

Figure 3: Precision of HGRNN-BES and existing approaches

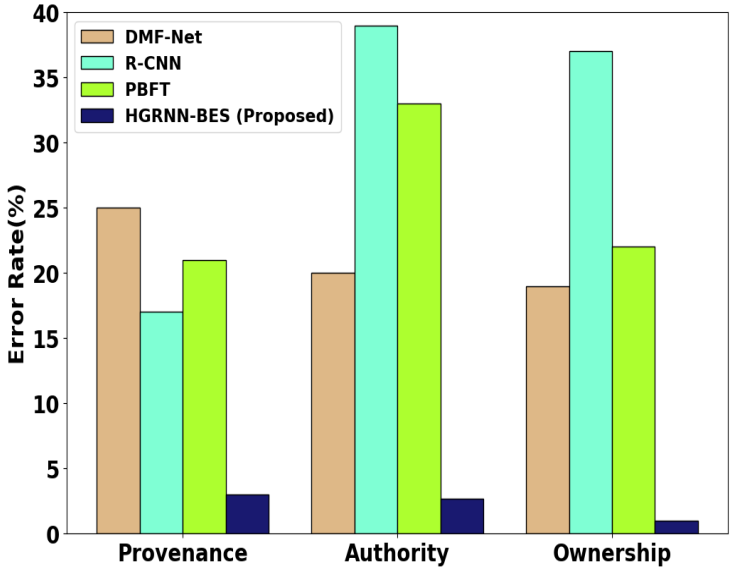

Figure 4: Error Rate of HGRNN-BES and existing approaches

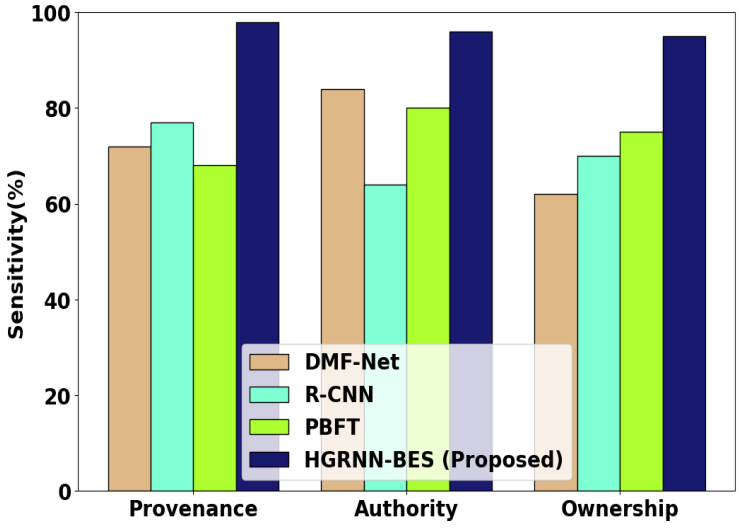

Figure 5: Sensitivity of HGRNN-BES and existing approaches

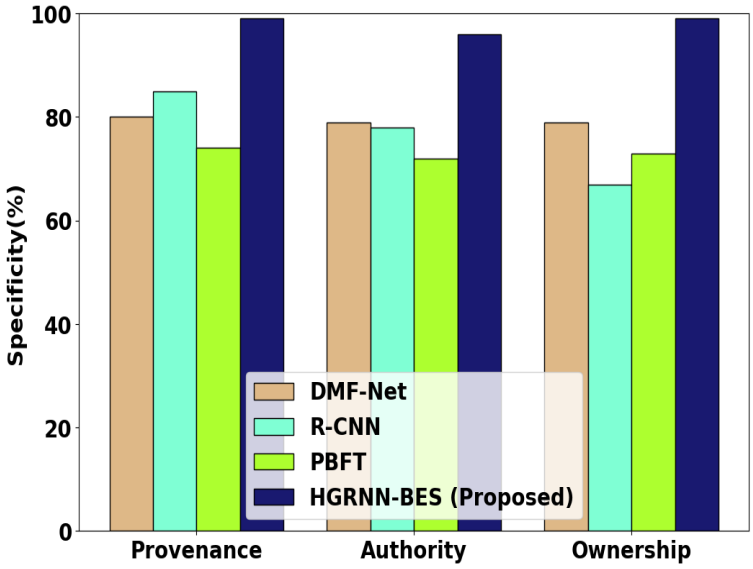

Figure 6: Specificity of HGRNN-BES and existing approaches

The sensitivity of DMF-Net approach is given as 70% in provenance and 82% in authority and 60% in ownership. The sensitivity of R-CNN is analyzed as 75% in provenance and 60% in authority and 70% in ownership. The sensitivity of PBFT is analyzed as 70% in provenance and 78% in authority and 72% in ownership. In our proposed method HGRNN-BES obtains 98% in provenience and 96% in authority and 95% in ownership it is shown in Figure 5. The specificity of DMF-Net approach is given as 80% in provenance and 78% in authority and 78% in ownership. The specificity of R-CNN is analyzed as 83% in provenance and 60% in authority and 70% in ownership. The specificity of PBFT is analyzed as 73% in provenance and 70% in authority and 72% in ownership. In our proposed method HGRNN-BES obtains 99% in provenience and 97% in authority and 99% in ownership it is shown in Figure 6.

V. CONCLUSION

In conclusion, this research based on block chain technology for Artwork Traceability and Anti-Counterfeiting Model based HGRNN and BES. One significant strategy to boost the growth of the art industry and increase artists' passion is through the Artworks anti-counterfeiting system. Theoretical investigation revealed that this method was extremely secure and efficient, and it can successfully stop information coding using block chain technology. The system has better security and less computational latency, according to the results. The proposed strategy lowers transaction latency and network connection expenses while enhancing system performance and throughput to satisfy high concurrency requirements for art work security traceability. The accuracy of the proposed HGRNN-BES approach gets accuracy is 99% and precision is 99%. The error rate of the proposed approach gets 2%. The existing approaches get lower performance than the proposed approaches.

Acknowledgements

Zhejiang Province Vocational Education "14th Five Year Plan" Teaching Reform Project（jg2023030）

REFERENCES

[1] Nguyen, D. C., Hosseinalipour, S., Love, D. J., Pathirana, P. N., & Brinton, C. G. (2022). Latency optimization for blockchain-empowered federated learning in multi-server edge computing. *IEEE Journal on Selected Areas in Communications*, *40*(12), 3373-3390.

[2] Shao, Q., Jin, C., Zhang, Z., Qian, W., & Zhou, A. (2018). Blockchain technology: architecture and progress. *Chinese Journal of Computers*, *41*(05), 969-988.

[3] Lu, Y., Li, P., & Xu, H. (2022). A Food anti-counterfeiting traceability system based on Blockchain and Internet of Things. *Procedia Computer Science*, *199*, 629-636.

[4] WANG, K., CHEN, Z., & XU, J. (2019). Efficient traceability system for quality and safety of agricultural products based on consortium blockchain. *Journal of Computer Applications*, *39*(8), 2438.

[5] Zhu, X. (2019, July). Research on blockchain consensus mechanism and implementation. In *IOP Conference Series: Materials Science and Engineering* (Vol. 569, No. 4, p. 042058). IOP Publishing.

[6] Linoy, S., Stakhanova, N., & Matyukhina, A. (2019, October). Exploring Ethereum's blockchain anonymity using smart contract code attribution. In *2019 15th International Conference on Network and Service Management (CNSM)* (pp. 1-9). IEEE.

[7] Chen, L., Lee, W. K., Chang, C. C., Choo, K. K. R., & Zhang, N. (2019). Blockchain based searchable encryption for electronic health record sharing. *Future generation computer systems*, *95*, 420-429.

[8] Chen, B., Wu, L., Wang, H., Zhou, L., & He, D. (2019). A blockchain-based searchable public-key encryption with forward and backward privacy for cloud-assisted vehicular social networks. *IEEE Transactions on Vehicular Technology*, *69*(6), 5813-5825.

[9] Mohan, A. P., & Gladston, A. (2020). Merkle tree and blockchain-based cloud data auditing. *International Journal of Cloud Applications and Computing (IJCAC)*, *10*(3), 54-66.

[10] Yang, F., Zhou, W., Wu, Q., Long, R., Xiong, N. N., & Zhou, M. (2019). Delegated proof of stake with downgrade: A secure and efficient blockchain consensus algorithm with downgrade mechanism. *IEEE access*, *7*, 118541-118555.

[11] Fazlali, M., Eftekhar, S. M., Dehshibi, M. M., Malazi, H. T., & Nosrati, M. (2019). Raft consensus algorithm: an effective substitute for paxos in high throughput p2p-based systems. *arXiv preprint arXiv:1911.01231*.

[12] Rui, Q., Shi, D., Qiang, W., & Qingxian, W. A. N. G. (2018). Blockchain Based Secure Storage Scheme of Dynamic Data [J]. *Computer science*, *45*(2), 57-62.

[13] Rehman Khan, S. A., Yu, Z., Sarwat, S., Godil, D. I., Amin, S., & Shujaat, S. (2022). The role of block chain technology in circular economy practices to improve organisational performance. *International Journal of Logistics Research and Applications*, *25*(4-5), 605-622.

[14] Shokri, A., Shokri, A., White, D., Gelski, R., Goldberg, Y., Harrison, S., & Rashidi, T. H. (2022). EnviroCoin: A Holistic, Blockchain Empowered, Consensus-Based Carbon Saving Unit Ecosystem. *Sustainability*, *14*(12), 6979.

[15] Rajawat, A. S., Goyal, S. B., Bedi, P., Simoff, S., Jan, T., & Prasad, M. (2022). Smart scalable ML-blockchain framework for large-scale clinical information sharing. *Applied Sciences*, *12*(21), 10795.

[16] Yang, K., Li, C., Jing, X., Zhu, Z., Wang, Y., Ma, H., & Zhang, Y. (2022). Energy dispatch optimization of islanded multi-microgrids based on symbiotic organisms search and improved multi-agent consensus algorithm. *Energy*, *239*, 122105.

[17] Xu, G., Bai, H., Xing, J., Luo, T., Xiong, N. N., Cheng, X., ... & Zheng, X. (2022). SG-PBFT: A secure and highly efficient distributed blockchain PBFT consensus algorithm for intelligent Internet of vehicles. *Journal of Parallel and Distributed Computing*, *164*, 1-11.

[18] Yu, Y., Liu, A., Dhawan, G., Mei, H., Zhang, W., Izawa, K., ... & Han, J. (2021). Fluorine-containing pharmaceuticals approved by the FDA in 2020: Synthesis and biological activity. *Chinese Chemical Letters*, *32*(11), 3342-3354.

[19] Guo, Z., Zheng, H., You, C., Wang, T., & Liu, C. (2022). DMF-Net: Dual-Branch Multi-Scale Feature Fusion Network for copy forgery identification of anti-counterfeiting QR code. *arXiv preprint arXiv:2201.07583*.

[20] Daoud, E., Vu, D., Nguyen, H., & Gaedke, M. (2019). Enhancing fake product detection using deep learning object detection models. *Universitat Chemnitz*.

[21] Tan, J., Goyal, S. B., Singh Rajawat, A., Jan, T., Azizi, N., & Prasad, M. (2023). Anti-Counterfeiting and Traceability Consensus Algorithm Based on Weightage to Contributors in a Food Supply Chain of Industry 4.0. *Sustainability*, *15*(10), 7855.

[22] Mohit, M., Kaur, S., & Singh, M. (2022). Design and implementation of transaction privacy by virtue of ownership and traceability in blockchain based supply chain. *Cluster computing*, 1-18.

[23] Alzahrani, N., & Bulusu, N. (2020). A new product anti-counterfeiting blockchain using a truly decentralized dynamic consensus protocol. *Concurrency and Computation: Practice and Experience*, *32*(12), e5232.

[24] Rajesh, M. (2021). Anti-counterfeiting and traceability mechanism based on blockchain. *Recent Trends in Intensive Computing*, *39*, 134.

[25] Tian, J., Hou, M., Bian, H., & Li, J. (2023). Variable surrogate model-based particle swarm optimization for high-dimensional expensive problems. *Complex & Intelligent Systems*, *9*(4), 3887-3935.

[26] Liu, M., Xie, Y., & Zhang, Y. L. (2013). Research on Ceramic Artworks' Anti-Counterfeiting and Authentication Based on Two-Dimensional Code. *Advanced Materials Research*, *791*, 2096-2099.

[27] Zhan, M., Zhao, C., Qin, K., Huang, P., Fang, M., & Zhao, C. (2023). Subaperture keystone transform matched filtering algorithm and its application for air moving target detection in an SBEWR system. *IEEE Journal of Selected Topics in Applied Earth Observations and Remote Sensing*, *16*, 2262-2274.

[28] Qin, Z., Yang, S., & Zhong, Y. (2024). Hierarchically gated recurrent neural network for sequence modeling. *Advances in Neural Information Processing Systems*, *36*.

[29] Marcilin, L., & Nandhitha, N. M. (2023). Design of Optical Filter Using Bald Eagle Search Optimization Algorithm. *Intelligent Automation & Soft Computing*, *36*(1).